cmgh
CELLULAR AND MOLECULAR GASTROENTEROLOGY AND HEPATOLOGY

ORIGINAL RESEARCH

Loss of Forkhead Box O3 Facilitates Inflammatory Colon Cancer: Transcriptome Profiling of the Immune Landscape and Novel Targets

Harrison M. Penrose,[1] Chloe Cable,[1] Sandra Heller,[1] Nathan Ungerleider,[1] Hani Nakhoul,[1] Melody Baddoo,[1] Alifiani B. Hartono,[1] Sean B. Lee,[1] Matthew E. Burow,[2] Erik F. Flemington,[1] Susan E. Crawford,[3] and Suzana D. Savkovic[1]

[1]Department of Pathology and Laboratory Medicine, Tulane University, New Orleans, Louisiana; [2]Department of Medicine, Section of Hematology and Medical Oncology, Tulane University Health Sciences Center, New Orleans, Louisiana; and [3]Department of Surgery, NorthShore University Research Institute, Affiliate of University of Chicago Pritzker School of Medicine, Evanston, Illinois

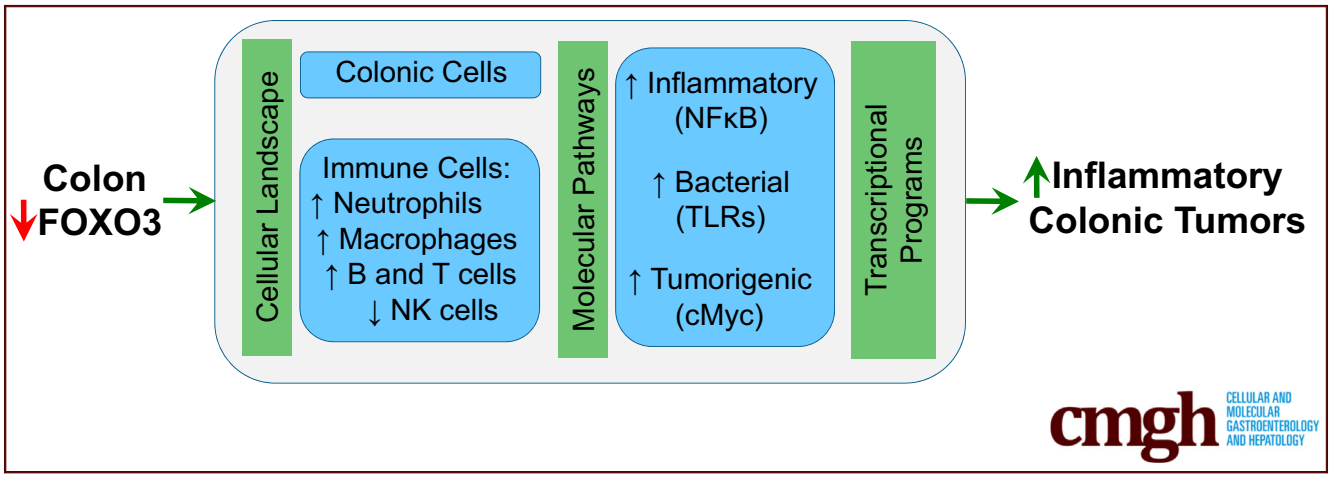

SUMMARY

Loss of FOXO3 transcription function, associated with human IBD and colon cancer progression, facilitates inflammatory colon cancer in mice. Transcriptome profiling of FOXO3 deficient colon and tumors revealed an immune landscape, molecular pathways, and novel transcripts similarly dysregulated in IBD and colon cancer.

BACKGROUND & AIMS: Diminished forkhead box O3 (FOXO3) function drives inflammation and cancer growth; however, mechanisms fostering these pathobiologies are unclear. Here, we aimed to identify in colon loss of FOXO3-dependent cellular and molecular changes that facilitate inflammation-mediated tumor growth.

METHODS: FOXO3 knockout (KO) and wild-type (WT) mice were used in the AOM/DSS model of inflammation-mediated colon cancer. Bioinformatics were used for profiling of mRNA sequencing data from human and mouse colon and tumors; specific targets were validated in human colon cancer cells (shFOXO3).

RESULTS: In mice, FOXO3 deficiency led to significantly elevated colonic tumor burden (incidence and size) compared with WT ($P < .05$). In FOXO3 KO colon, activated molecular pathways overlapped with those associated with mouse and human colonic inflammation and cancer, especially human colonic tumors with inflammatory microsatellite instability (false discovery rate < 0.05). FOXO3 KO colon, similar to tumors, had increased neutrophils, macrophages, B cells, T cells, and decreased natural killer cells (false discovery rate < 0.05). Moreover, in KO colon differentially expressed transcripts were linked to activation of inflammatory nuclear factor kappa B, tumorigenic cMyc, and bacterial Toll-like receptor signaling. Among differentially expressed transcripts, we validated altered expression of integrin subunit alpha 2 (ITGA2), ADAM metallopeptidase with thrombospondin type 1 motif 12, and ST8 alpha-N-acetyl-neuraminide alpha-2,8-sialyltransferase 5 in mouse WT and FOXO3 KO colon and tumors ($P < .05$). Similarly, their altered expression was found in human inflammatory bowel disease and colon cancer tissues and linked to poor patient survival. Ultimately, in human colon cancer cells, FOXO3 knockdown (shFOXO3) led to significantly increased ITGA2, and silencing ITGA2 (siRNA) alone diminished cell growth.

CONCLUSIONS: We identified the loss of FOXO3-mediated immune landscape, pathways, and transcripts that could serve as biomarkers and new targets for inflammatory colon cancer treatment. *(Cell Mol Gastroenterol Hepatol 2019;7:391–408; https://doi.org/10.1016/j.jcmgh.2018.10.003)*

Keywords: Colon Cancer; Inflammation; FOXO3; RNAseq.

See editorial on page 295.

Colon cancer, the second leading cause of cancer-related death in the United States, is driven by alterations in the tissue microenvironment caused by obesity, imbalances in the microbiome, and inflammation.[1–3] Local, chronic inflammation of the colon, as observed in inflammatory bowel disease (IBD), is associated with increased risk of cancer development and progression.[4,5] The inflammatory microenvironment initiates and fosters cancer progression as evident by its ability to stimulate transformed cell proliferation, survival, angiogenesis, metastasis, and resistance to chemotherapy.[1] Dynamic communication among cancer cells and the inflammatory microenvironment favors immune cell infiltration and the release of cytokines and growth mediators, both facilitators of cancer progression.[3] Furthermore, inflammation generated reactive nitrogen and oxidative species have been shown to mediate genetic instability in cancer cells.[1] In the colon, inflammation-mediated genetic microsatellite instability (MSI) favors an increased mutation rate leading to cancer progression.[1,6] However, the nature of the immune cell types, inflammatory mediators, and transcriptional programs that drive inflammation-mediated colon cancer are neither fully examined nor understood.

Transcription factor FOXO3, a member of the forkhead box O (FOXO) family, plays critical roles in diverse cellular functions including proliferation, apoptosis, and metabolism.[7,8] In immune cells, FOXO3 activity is critical for maintenance of immune progenitor cell homeostasis,[9,10] and its deficiency in B and T cells leads to their enhanced activity during infection.[11] In patients with inflammatory diseases such as rheumatoid arthritis and IBD, genome-wide association studies have shown that individuals with a single nucleotide polymorphism (SNP) in the FOXO3 gene locus leading to lowered FOXO3 expression have a more aggressive disease course.[12] Moreover, in human colon cancer tissues loss of FOXO3 transcription activity is associated with tumor growth.[13] Previously, we demonstrated that mice deficient in FOXO3 have increased susceptibility to colonic inflammation and elevated rates of cell proliferation.[14,15] Thus, we hypothesized that FOXO3's immunosuppressive and tumor-suppressive functions might intersect to drive inflammation-mediated colon cancer. Here, we aimed to determine loss of FOXO3-dependent changes in the immune landscape, molecular pathways, and downstream transcripts involved in disease pathobiology.

We demonstrated that in a mouse model of inflammation-mediated colon cancer FOXO3 deficiency led to increased tumor burden, an altered immune cell landscape, activated molecular pathways, and transcriptional programs associated with inflammation and tumor growth. Our analysis identified FOXO3-dependent transcripts that could potentially serve as biomarkers and prospective new targets for treatment.

Materials and Methods

Animals

Wild-type (WT) and FOXO3 knockout (FOXO3 KO) mice on a C57BL/6 genetic background[11] were housed at the Tulane University School of Medicine, a pathogen-free facility in static, microisolator caging. Homozygous littermates were offspring of heterozygous breeders and genotyped as described by Lin et al.[11] All experiments were completed according to guidelines and procedures determined by the Tulane Institutional Animal Care and Use Committee.

Azoxymethane and Dextran Sulfate Sodium Treatment

Mice, 6–8 weeks old, were injected intraperitoneally with a single dose (10 mg/kg) of azoxymethane (AOM) (Sigma-Aldrich, St Louis, MO; A5486) and subsequently administered 3 cycles of 2.5% dextran sulfate sodium (DSS) (MP Biomedicals, Santa Ana, CA; 160110) in drinking water for 5 days with 3-week intervals between each treatment regimen.[16] After 8 weeks of recovery, mice were killed, and colonic tissues were collected for analysis. Tumor counts and measurements were conducted in a blinded fashion.

Cell Culture and Generation of Short Hairpin RNA Stable Cell Lines

Human colon cancer HCT116 cells (ATCC) were grown in complete McCoy's 5A medium (Corning, Corning, NY; 10050CV) supplemented with 10% fetal bovine serum (Gibco Laboratories, Gaithersburg, MD; A3160602). For generating stable short hairpin RNA (shRNA) knockdown cell lines, FOXO3-specific shRNA (shFOXO3) and control shRNA were cloned into the TET-ON all in one LT3GEPIR vector[17] by using the following nucleotide shRNA guide sequences: 5′-CATGTTCAATGGGAGCTTGGA-3′ (shFOXO3),

Abbreviations used in this paper: **ADAMTS12, ADAM metallopeptidase with thrombospondin type 1 motif 12; AOM, azoxymethane; CIBERSORT, cell-type identification by estimating relative subsets of RNA transcripts; DE, differentially expressed; DSS, dextran sulfate sodium; FDR, false discovery rate; FOXO3, forkhead box O3; GSEA, gene set enrichment analysis; IBD, inflammatory bowel disease; IPA, ingenuity pathways analysis; ITGA2, integrin subunit alpha 2; KO, knockout; MMP, matrix metalloproteinase; MSI, microsatellite instability; NFκB, nuclear factor kappa B; NK, natural killer; PRECOG, prediction of clinical outcomes from genomic profiles; qPCR, quantitative polymerase chain reaction; RNAseq, mRNA sequencing; shRNA, short hairpin RNA; SNP, single nucleotide polymorphism; ST8SIA5, ST8 alpha-N-acetyl-neuraminide alpha-2,8-sialyltransferase 5; TCGA, The Cancer Genome Atlas; TIMER, Tumor Immune Estimation Resource; TLR, Toll-like receptor; TPM, transcripts per million; WT, wild-type.**

Most current article

2352-345X
https://doi.org/10.1016/j.jcmgh.2018.10.003

5′-TAGATAAGCATTATAATTCCTA-3′ (shCon). Sequence verified plasmids were transfected into HCT116 cells by using lipofectamine 3000 according to manufacturer's instructions (Invitrogen, Carlsbad, CA; L3000001). Stable cell lines were generated from single cells by using puromycin selection (250 ng/mL; Sigma-Aldrich; P8833), and doxycycline-inducible (2 μg/mL; Sigma-Aldrich; D9891) knockdown of FOXO3 was validated by quantitative polymerase chain reaction (qPCR) and immunoblot.

Small Interfering RNA

Human colon cancer HCT116 cells were transfected with integrin subunit alpha 2 (ITGA2) specific pooled small interfering RNA (Sigma-Aldrich; EHU040531) or equal amounts of negative-control scramble oligonucleotides using lipofectamine 3000 according to manufacturer's instructions (Invitrogen; L3000001). Efficiency of the knockdown was validated by qPCR and immunoblot.

Protein Extraction and Immunoblotting

Experimental cells were used for protein extraction, and immunoblot was performed as described previously.[14,18] The following specific antibodies against proteins were used: FOXO3 (Cell Signaling Technology, Danvers, MA; cat 2497, lot 8), ADAM metallopeptidase with thrombospondin type 1 motif 12 (ADAMTS12) (Abcam, Cambridge, United Kingdom; cat 203012, lot GR2390174; Thermo Scientific, Waltham, MA; cat PA568084, lot SK2479822E), ITGA2 (Abcam; cat 133557, lot GR19622312), ST8 alpha-N-acetyl-neuraminide alpha-2,8-sialyltransferase 5 (ST8SIA5) (Abcam; cat 184777, lot GR2231323), and β-actin (Cell Signaling Technology; cat 3700, lot 8). Proteins were visualized with IRDye-conjugated secondary antibodies (LI-COR Biotechnology, Lincoln, NE; goat anti-mouse, cat 92532210, lot C6072602; goat anti-rabbit, cat 92568071, lot 92632210) using the Odyssey infrared imaging system (LI-COR Biotechnology).

Cell Proliferation Assays

Human colon cancer HCT116 cells were plated on 96-well plates at a density of 5000 cells per well. After 72 hours, a portion of cell medium was removed, and MTS solution (Promega, Madison, WI; M3001) was added for 1 hour and incubated at 37°C. MTS-converted formazan product was detected in cell medium solution at 490 nm by using a Microplate Reader FLUOstar Optima (BMG Labtech, Ortenberg, Germany). Cell proliferation was calculated as a percentage of the absorbance relative to untreated control cells.

RNA Isolation and cDNA Synthesis

Human colon cancer cells and mouse tissues (colon and tumors) were used for isolation of total RNA by using the miRNeasy kit (Qiagen, Hilden, Germany; 217004) according to manufacturer's instructions. RNA quality was determined by an Agilent Bioanalyzer (Agilent Technologies, Santa Clara, CA), and samples with RNA integrity numbers (RIN) >7 were used. For qPCR, RNA treated with DNase was reverse transcribed to cDNA with oligo-dT12-18 primers of the SuperScript First-Strand Synthesis System (Invitrogen; 11904018) according to the manufacturer's protocol.

Quantitative Polymerase Chain Reaction

The cDNA generated from mouse tissues and human colon cancer cells was used for qPCR as previously described.[19,20] The following primers (Thermo Fisher Scientific) were used for amplification of human and mouse cDNA: Itga2 (human: hItga2-FOR 5′-GGTGCTCCTCGGGCAAATTA-3′, hItga2-REV 5′-GAGCCAATCTGGTCACCTCG-3′; mouse: mItga2-FOR 5′-TGGTAGTTGTGACCGATGGC-3′; mItga2-REV 5′-ACCC AAGAACTGCTATGCCG-3′), Adamts12 (mAdamts12-FOR 5′-CTGCCAAGGACTGACTGGATT-3′, mAdamts12-REV 5′-GTAG GACCCTTCCTCGGTCA-3′), St8sia5 (mSt8sia5-FOR 5′-CTTGT CCAGGTGCTGCAATG-3′; mSt8sia5-REV 5′-AGGGCATTTCCTTG GGAAACA-3′), Tlr4 (mTlr4-FOR 5′-AATCCCTGCATAGAGGT AGTTCC-3′, mTlr4-REV 5′-ATCCAGCCACTGAAGTTCTGA-3′), FOXO3 (hFoxo3-FOR 5′-TGGTTTGAACGTGGGGAACT-3′, hFoxo3-REV 5′-GTGTCAGTTTGAGGGTCTGCT-3′). To determine the relative levels of mRNA the comparative Ct method was used with Hprt-1 as a housekeeping control. The C1000 Thermal Cycler system (Bio-Rad, Hercules, CA) and iQ SYBR Green DNA double-strand binding dye (iQ SYBR Green Supermix; Bio-Rad; 1708885) were used to quantify cDNA. As expected, PCR amplification was unaffected in mouse colonic tumors because of ample time between the last DSS treatment and RNA extraction.[21]

RNA Sequencing and Differential Expression Testing

RNA sequencing (RNAseq) and differential expression testing were accomplished as described previously.[19,20] Specifically, RNAseq and library preparation was completed by University of Wisconsin Biotechnology Facility (http://www.biotech.wisc.edu/services/dnaseq). The mRNA was enriched via poly-A selection (1 μg input per sample), and the Illumina Truseq Stranded mRNA preparation kit was used for library preparation (Illumina Inc, San Diego, CA). After cDNA synthesis, indexing adapters were ligated to ends of cDNA, and PCR enrichment of DNA fragments with adapters was performed. Library quality, profile, and size were validated by using an Agilent DNA 1000 Chip (Agilent Technologies). One hundred base-pair strand-specific RNAseq was performed on validated samples by using Illuming HiSeq 2500 technology (Illumina Inc). Bioinformatics analyses of raw RNAseq data were performed in the Tulane Cancer Center Next Generation Sequence Analysis core (www.tulane.edu/som/cancer/research/core-facilities/cancer-crusaders). RNAseq reads were mapped to the mouse reference haploid genome sequence (Genome Reference Consortium murine genome build 38, GRCm38). Quantification of transcript expression was accomplished by using the software package RSEM (v1.2.25). Subsequent identification of differentially expressed (DE) transcripts at the whole gene level between biological conditions was performed by using EBseq and attained with a false discovery rate (FDR) of 0.05. Sequencing data along with the study design have been submitted in NCBI's Sequence Read Archive and are available under study accession number SRP158292.

Transcriptome and Pathway Analysis

Networks, functional analysis, and interpretation of RNAseq data were performed by using Ingenuity Pathway Analysis (IPA) (Qiagen Inc). Transcripts entered into IPA met an expression threshold of >|1.5|-fold change with respect to control and an FDR <0.05. Transcriptional signatures from our samples were compared against available gene expression data from mouse colon with inflammation or dysplasia as well as human IBD and colon cancer samples using NCBI's GEO2R after adjustment with Benjamini and Hochberg testing ($P < .05$).[22] In addition, our transcriptional signatures were compared against

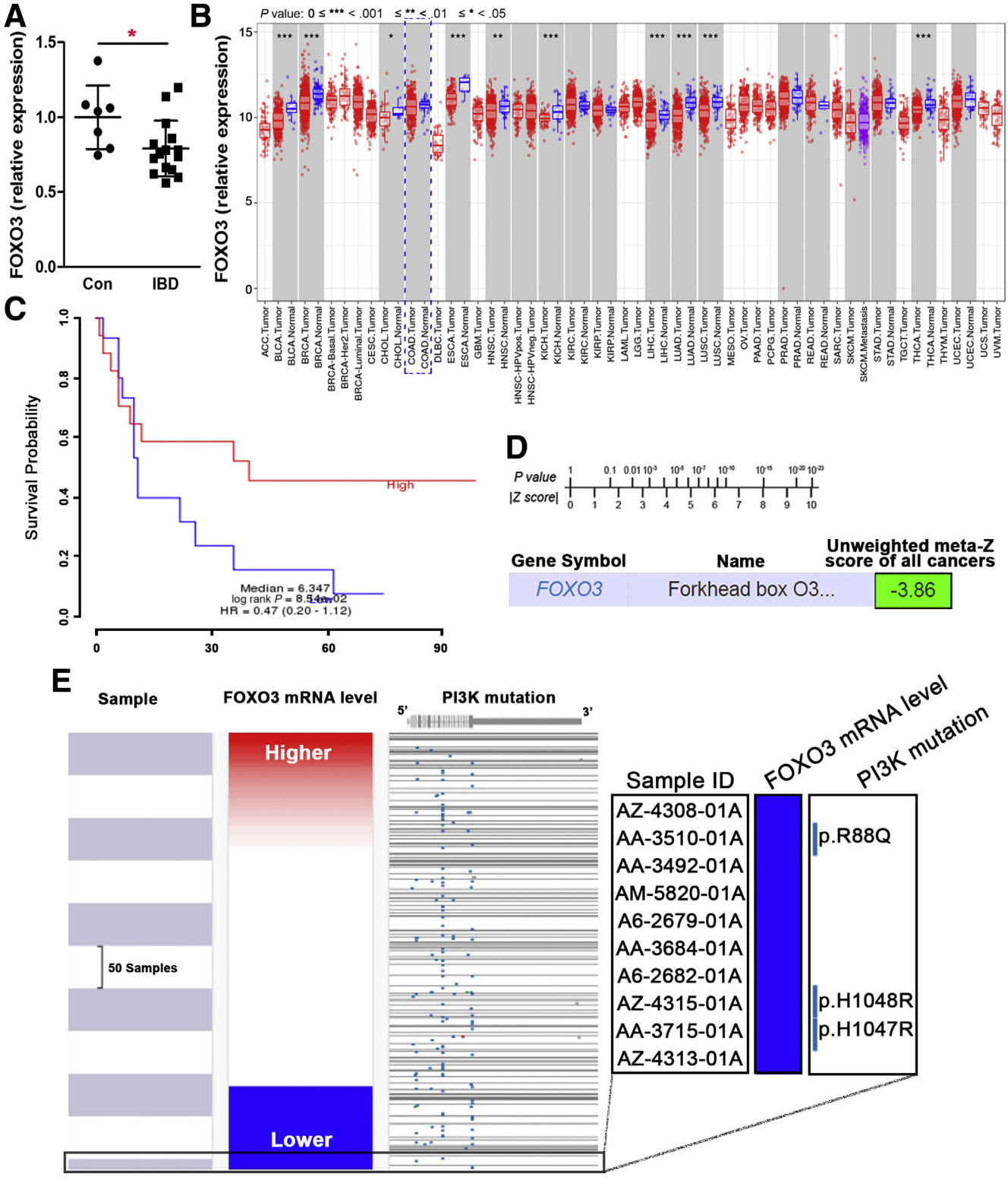

transcriptomes from human colon cancer tissue (The Cancer Genome Atlas [TCGA]) by using Firebrowse.[23]

cBioPortal for Cancer Genomics

Investigation of transcript dysregulation in human colon cancer samples was analyzed by using the cBioPortal for Human Cancer Genomics[24,25] (www.cbioportal.org). Selected genes in human colorectal adenocarcinoma patient samples (TCGA COAD) were analyzed by using a z-score threshold of ±2 for RNAseq analyses for all tumors as quantified by RSEM (RNAseq by Expectation Maximization)[26]; Case Set: All Tumors (631 patients/636 samples)).

Cell-type Identification by Estimating Relative Subsets of RNA Transcripts

To identify the immune cell landscape in a mixed colonic tissue sample, the computational cell-type identification by estimating relative subsets of RNA transcripts (CIBERSORT) method was applied to RNAseq data.[27] Mixture files were created by using transcripts per million (TPM) from RNAseq samples according to the CIBERSORT formatting requirements (http://cibersort.stanford.edu). For mouse immune and colonic cells, a custom gene signature, reference, and phenotype file were created in accordance with CIBERSORT format specifications using the following RNA-seq run accession numbers: B cells (SRR1976588, SRR1976593, SRR3932662, SRR3932664), CD4 T cells (SRR1976591, SRR3932665), CD8 T cells (SRR3001784, SRR3001786, SRR3001782), macrophages (SRR1976597, SRR3932663, SRR2927689), neutrophils (SRR1177062, SRR1177063, SRR3932667, SRR1976571), natural killer (NK) cells (SRR1976589, SRR3932669, SRR1976596, SRR3932670), and colonocytes (SRR3189717 [ATCC CMT-93 cells], SRR3189714 [1638NT1 cells]). Only those values meeting a significance threshold of $P < .05$ were included in analysis.

Tumor Immune Estimation Resource

Tumor immune estimation resource (TIMER) was used to assess mRNA expression in human cancer relative to normal matched tissue (RNAseq RSEM, TCGA)[28] (https://cistrome.shinyapps.io/timer/).

Gene Set Enrichment Analysis

Gene set enrichment analysis (GSEA) software and the Molecular Signature Database were used to determine activation of transcription factor targets from RNAseq data.[29]

Histologic Analysis

Mouse tissue processing and immunohistostaining were performed by the Pathology Core Laboratory at Tulane University Health Sciences Center (http://medicine.tulane.edu/departments/pathologylaboratorymedicine/research/histology-laboratory) as described previously.[19,20] Heat-induced epitope retrieval was performed on tissue sections by using Rodent Decloaker solution (BioCare Medical, Concord, CA; RD913) and cooked in an oster steamer for 40 minutes. Sections were blocked by using Rodent Block M (BioCare Medical; RBM961), followed by incubation with the following antibodies: ADAMTS12 (Abcam; cat 203012, lot GR2390174), ITGA2 (Abcam; cat 133557, lot GR19622312), ST8SIA5 (Abcam; cat 184777, lot GR2231323), and Ki67 (1:100, 45 minutes; BioCare Medical; CRM325). After washing, tissue sections were incubated with Rabbit-on-Rodent HRP-Polymer secondary (BioCare Medical; RMR622); sections were then washed and treated with Betazoid DAB chromogen (Biocare Medical; BDB2004), followed by counterstaining with Cat hematoxylin (Biocare Medical; CATHEM). Slides were dried in the oven, placed in xylene, and coverslipped (Acrymount; StatLab, McKinney, TX; SL804). Images were obtained by using the slide scanner Aperio CS2 (Leica, Wetzlar, Germany) and Image Scope software.

Statistical Analysis

All data are means ± standard deviation for a series of experiments. Statistical analysis was performed by Student unpaired *t* test or one-way analysis of variance and Student-Newman-Keuls post-test by using Graph Pad Instat 3 software (Graphpad Software, San Diego, CA). A P value $<.05$ was considered significant.

Results

In Mouse Colon, Forkhead Box O3 Deficiency Leads to Increased Tumor Burden and Activates Pathways Associated With Inflammation and Cancer

Because reduced FOXO3 transcription function has been linked to severity of human IBD and colon cancer pathobiology,[12,13] we assessed how loss of its activity might contribute to inflammation-mediated colon tumor

Figure 1. (***See previous page***). **In human IBD and cancer, FOXO3 mRNA levels are reduced and associated with poor survival and partial PI3K activating mutations.** (*A*) In human IBD tissue samples, relative expression (microarray) of FOXO3 transcript was significantly reduced compared with normal matched control tissue (GSE4183, n = 23; Affymetrix probe ID: 204131_s_at; *$P < .05$, IBD compared with normal colon, Student *t* test). (*B*) mRNA expression (RNAseq, RSEM) of FOXO3 across TCGA cohorts (TIMER, https://cistrome.shinyapps.io/timer/). (*C*) Representative Kaplan-Meier survival plot demonstrating decreased FOXO3 mRNA expression is associated with reduced colon cancer patient survival (GSE16125, n = 32; https://precog.stanford.edu/index.php). (*D*) PRECOG meta-z analysis indicating increased FOXO3 expression as prognostic for favorable overall cancer survival ($P < .05$, https://precog.stanford.edu/index.php). (*E*) In human colon cancer (TCGA), the 10 patients expressing the lowest FOXO3 mRNA (compared with average FOXO3 level in tumor) (RNAseq, HTseq) and their 3 (p.H1047R, p.H1048R, p.R88Q) corresponding PI3K activating mutations (MuTect2 Variant Browser) (UCSC Xena Genome Browser, http://xena.ucsc.edu).

progression. Initially, analysis of transcriptomes from patients with IBD (microarray) and colon cancer tissues (microarray and RNAseq) revealed decreased FOXO3 expression across both pathologies (Figure 1*A* and *B*). Compared with matched normal tissue, FOXO3 transcript levels were also decreased in approximately 60% of other cancers (TCGA) (Figure 1*B*). In addition, reduced FOXO3 in human colon cancer was linked to poor patient survival as assessed by KM estimate (Figure 1*C*), which was further supported by pan-cancer meta-z analysis demonstrating increased FOXO3 expression as a favorable prognostic indicator in cancer survival (Stanford, prediction of clinical outcomes from genomic profiles [PRECOG]) (Figure 1*D*). Last, we determined in human colon cancer tissues (TCGA) whether low FOXO3 expression was associated with increased PI3K activity, which is known to negatively regulate FOXO3[30] and favor cancer progression.[31] In patients with the lowest FOXO3 transcript levels, 3 of 10 had PI3K activating mutations (UCSC, XENA) (Figure 1*E*), suggesting that in human colon cancer loss of FOXO3-

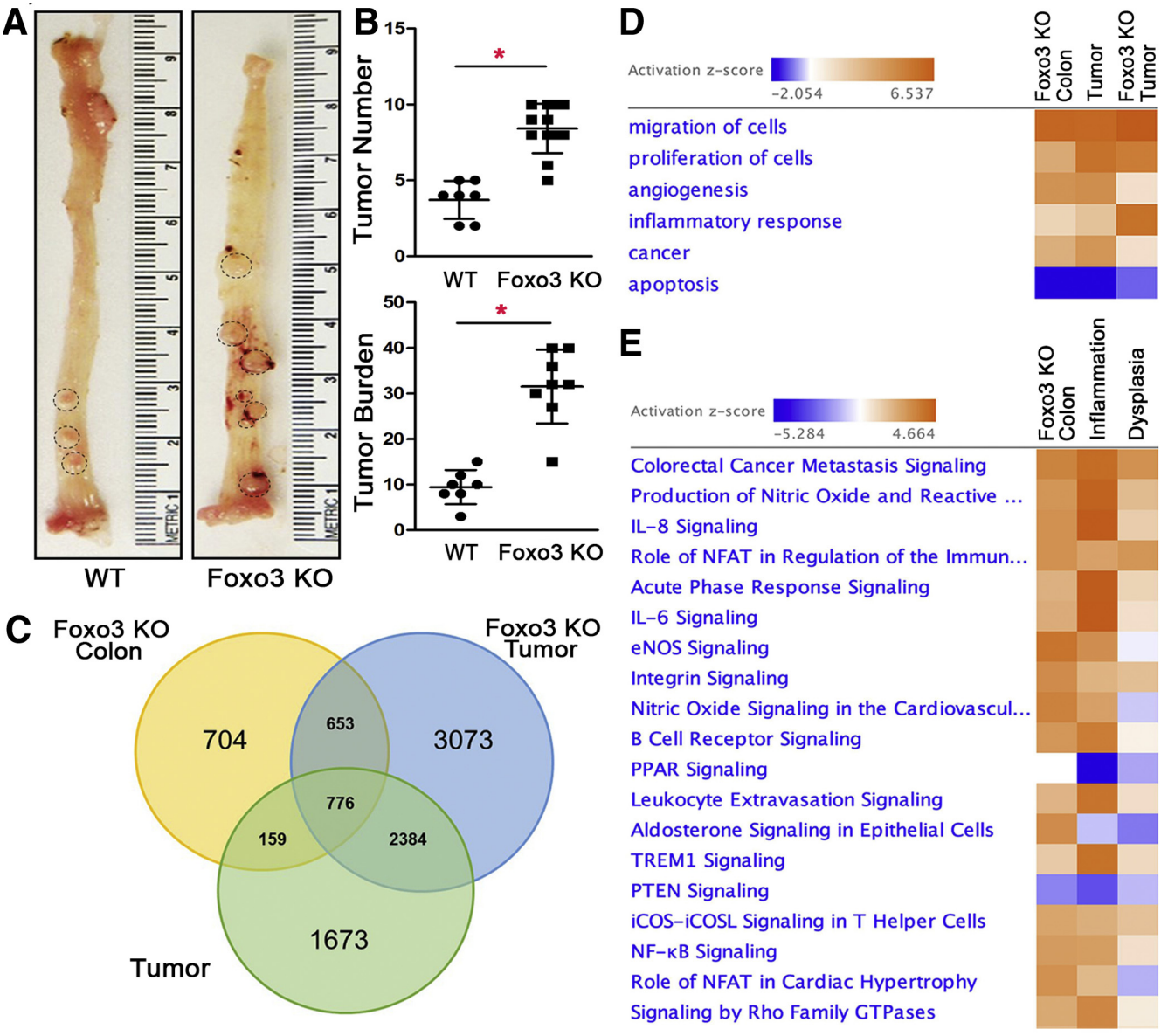

Figure 2. In mouse colon FOXO3 deficiency increases colonic tumor burden and activation of inflammatory and tumorigenic transcriptional programs. (*A* and *B*) Gross histology of WT and FOXO3 KO colonic tumors in the AOM/DSS mouse model. Colonic tumor incidence, size, and tumor burden were determined between WT and FOXO3 KO (n = 8 per experimental group, representative graph from 2 independent experiments; *$P < .05$ compared with WT, Student *t* test). (*C*) Venn diagrams depict the number of transcripts commonly or uniquely expressed in mouse FOXO3 KO colon and tumors (WT or KO in AOM/DSS model) relative to WT (n = 3 per experimental group, FDR < 0.05, EBseq). (*D*) Disease and function analysis of colonic FOXO3 KO transcriptome revealed association with inflammatory and cancer pathobiology (n = 3 per experimental group, FDR < 0.05, IPA). (*E*) Top canonical pathways activated in mouse FOXO3 KO colon (n = 6) compared with both mouse inflamed and dysplastic colonic tissue (GSE31106, n = 15) (FDR < 0.05, IPA).

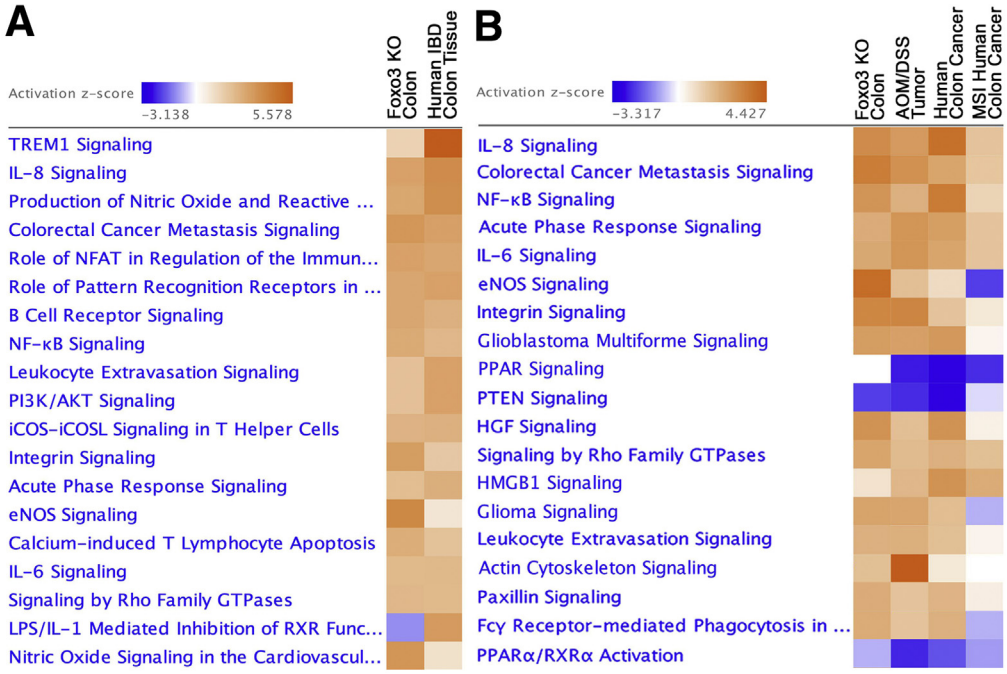

Figure 3. Loss of FOXO3 leads to altered transcript expression similarly observed in human intestinal inflammation and colon cancer. (*A*) Canonical pathway analysis revealed high degree of transcriptional similarity between mouse FOXO3 KO colon (n = 6) and human IBD (GSE4183, n = 23 patient samples) (FDR < 0.05, IPA). (*B*) Pathway analysis revealed that transcriptional signatures from mouse FOXO3 KO colon and AOM/DSS tumors shared high degree of similarity with human colon cancer, especially those with MSI (TCGA) (n = 3 per experimental group, FDR < 0.05, IPA).

mediated progression could be either PI3K-dependent or -independent. Together, these findings demonstrate that in human IBD and colon cancer, FOXO3 expression is reduced, in part, independently of upstream PI3K and associated with reduced patient survival.

By using KO mice, we assessed the loss of FOXO3-dependent transcriptional consequences that could facilitate inflammation-mediated cancer progression. In the AOM/DSS model, approximately one-third of FOXO3 KO mice displayed rectal prolapse; nevertheless, survival rates between WT and KO mice did not differ during the time of the experiment. Macroscopic examination of colon revealed that FOXO3 KO mice had a greater tumor incidence (2-fold) and size (>3 mm), leading to a significantly increased tumor burden (3-fold) compared with WT (Figure 2*A* and *B*). Microscopic assessment of tumors (H&E stained) for penetration of surrounding lamina propria or spreading to lymph nodes did not show differences between WT and FOXO3 KO, suggesting that in this model and for the duration of the experiment, cancer invasion and metastasis appear to be independent of FOXO3 deficiency. Next, RNAseq analysis showed in FOXO3 KO colon a significant number of DE transcripts were also shared with tumors (WT and FOXO3 KO) (Figure 2*C*). IPA of these DE transcripts indicated altered biological functions pertaining to tumor growth including increased cell migration, proliferation, angiogenesis, inflammation, cancer, and decreased apoptosis (Figure 2*D*). Moreover, the FOXO3 KO transcriptional signature displayed strong similarities with inflammatory and dysplastic transcriptomes of mouse colon (GSE31106) (Figure 2*E*), suggesting its functional deficiency might support both processes. Also, we found in FOXO3 KO colon that dysregulated pathways substantially overlapped with those altered in human IBD and colon cancer (GSE4183) (Figure 3). Particularly in KO colon and AOM/DSS tumors, IPA revealed gene expression was similar to transcriptomes from human colon cancers with MSI, characterized by an inflammatory tumor microenvironment (TCGA) (Figure 3*B*). These findings demonstrate that in mouse colonic tissue, FOXO3 deficiency increases tumor burden and promotes transcriptional changes similar to those occurring in human IBD and colon cancer, especially tumors with inflammatory MSI features.

In Mouse Colon, Forkhead Box O3 Deficiency Leads to an Altered Immune Cell Landscape Similar to Inflammatory Tumors

On the basis of the above findings and because loss of FOXO3 function is critical in mediating inflammatory and proliferative responses in both colonic and immune cells,[9,14,15] we applied CIBERSORT[27] to assess the relative abundance of immune cell types in experimental tissues. This program uses transcriptional signatures of distinct immune cell types to assess their presence in a mixed cell tissue by using RNAseq data.[27] Compared with WT mice, FOXO3 KO colon showed significantly increased levels of macrophages (2-fold), neutrophils (3-fold), and reduced NK cells (Figure 4*A*). Also, although both B cells and T cells (CD4 and CD8) were elevated in FOXO3 KO colon, only increases in B cells (3-fold) reached statistical significance (Figure 4*B*). This immune profile, similarly described in human inflammatory colon cancer,[3,32] was also seen in mouse AOM/DSS tumors (data not shown). Moreover, these findings were further supported by analysis of upstream pathways (IPA), which identified increased expression and activation of receptors and cytokines specific for the presence of macrophages (interleukin 1A, interleukin 1B)

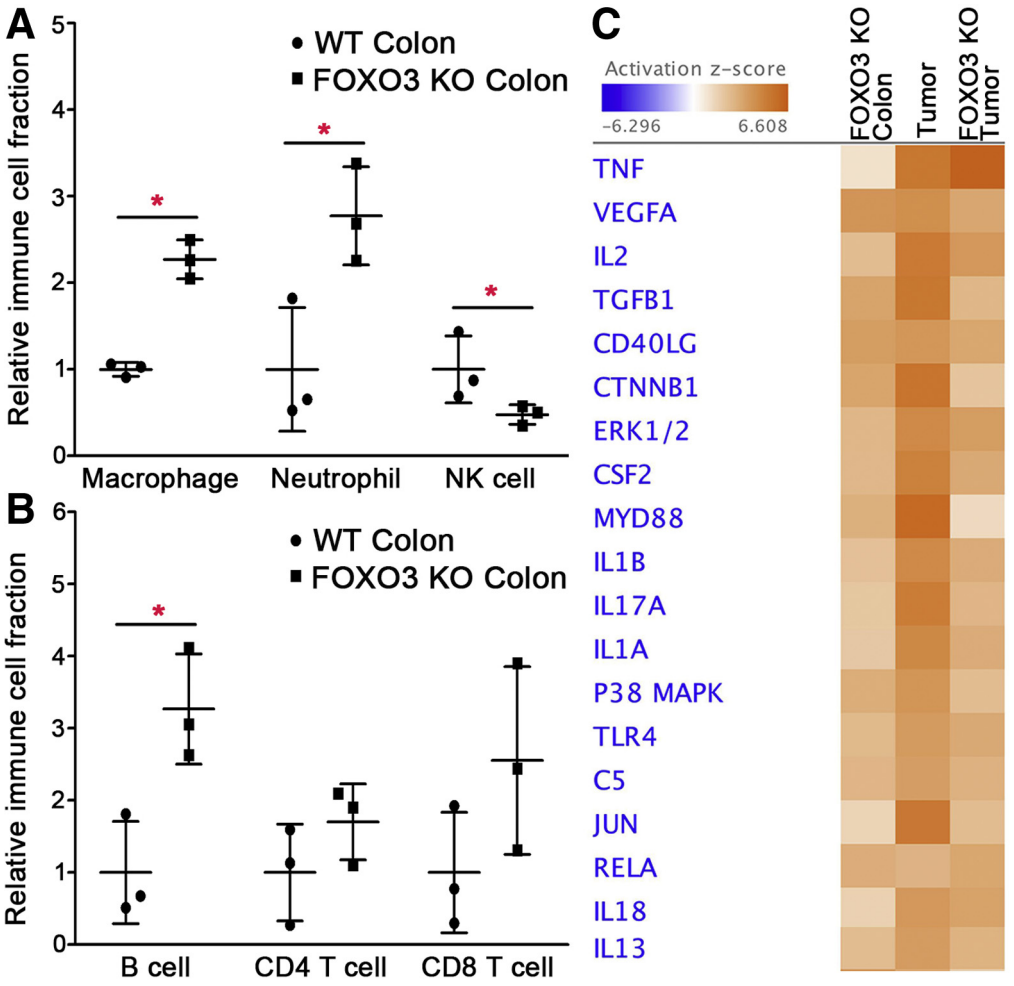

Figure 4. FOXO3 deficiency promotes infiltration of immune cells in mouse colon and tumor microenvironment. (*A* and *B*) CIBERSORT relative abundances of select immune cell infiltrate in FOXO3 KO colon relative to WT (fold-change) (n = 3 per experimental group; **P* < .05 compared with WT, analysis of variance and Student-Newman-Keuls post-test). (*C*) IPA upstream regulator analysis of FOXO3 KO colon and tumor (WT and KO) transcriptomes (n = 3 per experimental group, FDR < 0.05, IPA).

(Figure 4*C*), neutrophils (interleukin 8) (Figure 2*E*), B cells (receptor signaling) (Figure 2*E*), and T cells (interleukin 13, interleukin 17A) (Figure 4*C*). These data show that in colon and AOM/DSS tumors FOXO3 deficiency leads to an altered immune cell landscape and inflammatory microenvironment that could potentially support cancer progression.

In Mouse Colon, Forkhead Box O3 Deficiency Activates Transcriptional Programs Associated With Inflammation, Tumorigenesis, and Bacterial Signaling

Next, we determined loss of FOXO3-dependent transcripts that may influence inflammation and cancer. Initially, GSEA recognized a prevalent number of FOXO3 DE transcripts as being regulated by inflammatory nuclear factor kappa B (NFκB) and tumorigenic cMyc transcription factors (Figure 5*A*). Moreover, among FOXO3 KO DE transcripts that were shared with AOM/DSS tumors (Figure 2*C*), we selected 50 novel transcripts (Table 1) that could play a potential role in colon cancer. IPA also demonstrated numerous elevated DE transcripts with biological roles in inflammation and cancer progression (Figure 5*B*) including S100A8, Wnt ligands, and several matrix metalloproteinases (MMPs).[33–35] Furthermore, the transcriptome of FOXO3 KO colon displayed activated signals specific for bacterial factor(s) recognition including Toll-like receptors TLR4, TLR7, TLR8, and their downstream transducer MYD88 (Figures 4*C* and 5*B*). In particular, significant up-regulation of TLR4 expression (2.5-fold) was validated by qPCR in FOXO3 KO colon (Figure 5*C*). Several of these TLRs, expressed in colonic cells and antigen presenting cells, are associated with increased susceptibility to developing intestinal inflammation and cancer.[36,37] These findings identify loss of FOXO3-dependent transcripts that have established and potential roles in inflammation and tumor growth.

Altered Expression of Novel Integrin Subunit Alpha 2, ADAM Metallopeptidase With Thrombospondin Type 1 Motif 12, and ST8 Alpha-N-Acetyl-Neuraminide Alpha-2,8-Sialyltransferase 5 Transcripts in Mouse and Human Colon and Tumors

Because our bioinformatics revealed FOXO3 deficiency altered transcripts that were also dysregulated in tumors,

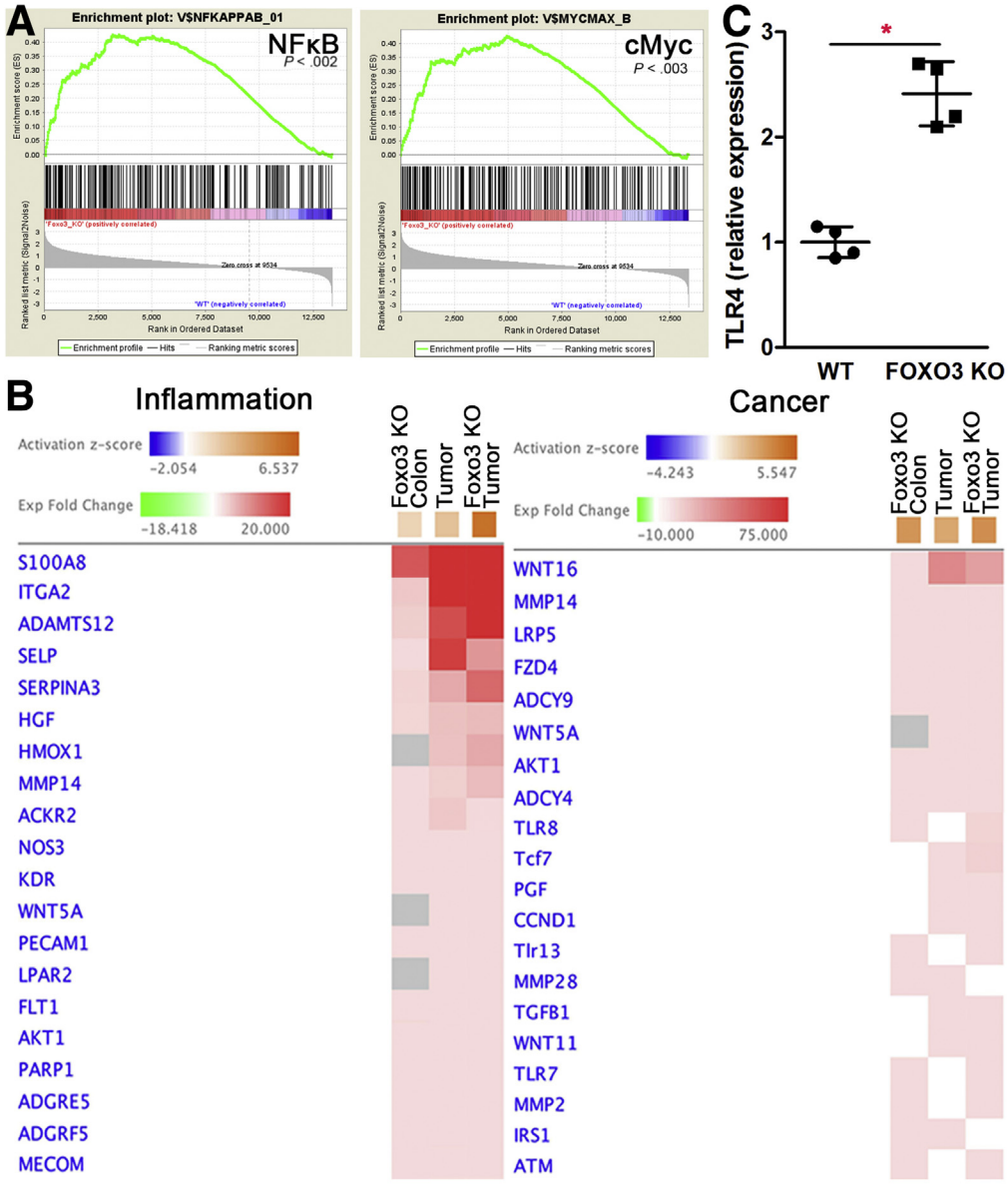

Figure 5. In mouse colon FOXO3 deficiency leads to activation of transcriptional programs associated with inflammation, tumorigenesis, and bacterial signaling. (*A*) GSEA of FOXO3 KO colon transcriptome revealed activation of inflammatory and tumorigenic transcriptional motifs (n = 6, **P* < .05). (*B*) Heatmap profiling revealed transcripts significantly elevated in FOXO3 KO colon and tumors (WT and KO) from inflammatory and cancer signaling (n = 3 per experimental group, FDR < 0.05, IPA). (*C*) Total RNA was extracted from WT or FOXO3 KO colon, and TLR4 mRNA levels were quantified by using qPCR (n = 4 per group from 2 independent experiments; **P* < .05 compared with WT colon, Student *t* test).

we used molecular approaches to validate expression of select DE transcripts in FOXO3 KO colon and tumors (WT and KO). Among transcripts positively or negatively dependent on FOXO3, we selected those genes (significantly DE) with diverse functions and select abundances in colonic and non-colonic cells. Specifically, we validated ITGA2, a membrane and intracellular integrin family member highly expressed in the colon,[38] ADAMTS12, an extracellular and intracellular metallopeptidase family with expression in colonic and non-colonic cells,[39] and ST8SIA5, a sialyltransferase involved in ganglioside synthesis, with low basal expression in the colon and possible localization to the Golgi.[40] Quantitative PCR and immunohistostaining showed significantly increased expression of ITGA2 and ADAMTS12 as well as decreased ST8SIA5 in FOXO3 KO colon and tumors relative to WT (Figure 6) confirming RNAseq data. In mouse WT colon, ITGA2 protein was present in colonic cells, mostly localized in the membrane of proliferative cells of the crypt, whereas in KO colon and tumors, its overall levels were considerably augmented. Also, in mouse WT colon, ADAMTS12 protein was localized in colonic cells (intracellular and membrane) along the crypt, whereas in FOXO3 KO colon and tumors, it was elevated in colonic but more noticeably in non-colonic cells. ST8SIA5 was present at lower levels in colonic cells, more so in upper parts of crypt cells potentially within vacuoles as evident by punctate staining. In FOXO3 KO colon and tumors, the amount of ST8SIA5 was diminished (Figure 6). Furthermore, as a positive control, tissues were stained for Ki67, which demonstrated an increased number of proliferative cells in FOXO3 KO colon relative to WT (Figure 6*B*), confirming our previous finding of increased proliferation in response to

Table 1. DE Transcripts in FOXO3 KO Colon Similarly Up- and Down-Regulated in Tumors (AOM/DSS)

Gene	Gene name	Colon FOXO3 KO	Tumor (AOM/DSS)
SGSM3	Small G protein signaling modulator 3	595.078	91.142
FAM103A1	Family with sequence similarity 103, member A1	565.122	152.628
ZBED6	Zinc finger, BED type containing 6	106.973	61.437
MCPT4	Mast cell protease 4	41.723	19.823
CFD	Complement factor D	33.03	7.816
ADIPOQ	Adiponectin, C1Q and collagen domain	30.559	10.799
LEP	Leptin	25.853	16.14
CPA3	Carboxypeptidase A3, mast cell	25.089	8.962
ARFIP1	ADP ribosylation factor interacting protein 1	20.479	3.18
S100A8[a]	S100 calcium binding protein A8	15.034	792.785
AMD1	S-adenosylmethionine decarboxylase 1	14.95	2.282
RBM12	RNA binding protein 12	12.773	11.412
MOAP1	Modulator of apoptosis 1	12.399	4.448
CHSY3	Chondroitin sulfate synthase 3	10.147	4.858
KLF12	Kruppel like factor 12	7.802	6.82
WNT16	Wnt family member 16	6.814	37.196
UPRT	Uracil phosphoribosyltransferase	6.174	2.941
LCOR	Ligand dependent nuclear receptor Corepressor	6.089	3.089
SYNE3	Spectrin repeat containing, nuclear envelope family member 3	5.691	1.515
PAPLN	Papilin, proteoglycan-like sulfated glycoprotein	5.62	3.152
CBL	Cbl proto-oncogene	5.582	2.108
LMBRD2	LMBR1 domain containing 2	5.479	2.988
LNPEP	Leucyl/cystinyl aminopeptidase	5.468	2.236
NT5C1A	5'-nucleotidase, cytosolic IA	5.194	3.413
ATP7A	ATPase, copper transporting alpha	5.098	3.102
CCDC85C	Coiled-coil domain containing 85C	4.92	2.431
PCOLCE2	Procollagen C-endopeptidase enhancer 2	4.846	1.806
SLFN5	Schlafen 5	4.763	3.99
SAMD12	Sterile alpha motif domain containing 12	4.647	5.439
ITGA2	Integrin alpha 2	4.356	20.059
EXPH5	Exophilin 5	4.348	2.457
PM20D2	Peptidase M20 domain containing 2	4.105	6.56
PTAR1	Protein prenyltransferase alpha subunit repeat containing 1	4.006	2.109
VPS13C	Vacuolar protein sorting 13C	4	1.736
ADAMTS12	ADAM metallopeptidase with thrombospondin type 1 motif 12	3.927	16.032
TCHH	Trichohyalin	3.897	5.262
XKR4	XK related 4	3.895	3.658
MIA2	Melanoma inhibitory activity 2	3.847	2.227
PDPR	Pyruvate dehydrogenase phosphatase regulatory subunit	3.784	1.999
PCDHGC3	Protocadherin gamma subfamily C, 3	3.771	3.844
IGFBP3[a]	Insulin-like growth factor binding protein 3	3.711	10.152
STON2	Stonin 2	3.64	1.98
ADAMTS3	ADAM metallopeptidase with thrombospondin type 1 motif 3	3.574	2.979
ARSB	Arylsulfatase B	3.568	1.626
TNKS	Tankyrase	3.502	2.947
SERPINA3	Serpin family A member 3	3.48	7.076
SLC25A30	Solute carrier family 25, member 30	3.436	4.609
SNX29	Sorting nexin 29	3.356	1.737
WDFY2	WD repeat and FYVE domain containing 2	3.308	3.602
LPAR5	Lysophosphatidic acid receptor 5	3.295	2.073

Table 1. Continued

Gene	Gene name	Colon FOXO3 KO	Tumor (AOM/DSS)
LENEP	Lens epithelial protein	–85.425	–69.786
USP9Y	Ubiquitin specific peptidase 9, y-linked	–42.229	–22.166
DDX54	DEAD box polypeptide 54	–21.688	–2.797
UGT1A4	UDP glucuronosyltransferase 1 family, polypeptide A4	–21.403	–14.754
LIPF	Lipase F	–9.735	–5.841
RPGRIP1	Retinitis pigmentosa GTPase regulator Interacting protein 1	–5.034	–3.058
RPL41	Ribosomal protein L41	–4.189	–2.691
CES3	Carboxylesterase 3	–3.743	–6.789
RAB33A	RAB33A, member RAS oncogene family	–3.669	–4.316
RGS1	Regulator of G-protein signaling 1	–3.665	–5.723
NTAN1	N-terminal Asn amidase	–3.566	–2.115
UGT1A1	UDP glucuronosyltransferase 1 family, polypeptide A1	–3.531	–2.425
UGT2B17	UDP glucuronosyltransferase family 2, member B17	–3.505	–3.248
MFSD9	Major facilitator superfamily domain containing 9	–3.397	–2.942
SPDYA	Speedy/RINGO cell cycle regulator family, member A	–3.128	–1.815
SLC17A1	Solute carrier family 17, member 1	–2.86	–2.822
CFAP52	Cilia and flagella associated protein 52	–2.763	–1.652
DPPA5	Developmental pluripotency associated 5	–2.698	–3.306
NR1I3	Nuclear receptor subfamily 1 group I member 3	–2.674	–6.541
SERPINC1	Serpin family C member 1	–2.57	–1.717
CDA	Cytidine deaminase	–2.547	–1.518
TAT	Tyrosine aminotransferase	–2.402	–3.944
NLRP9	NLR family pyrin domain containing 9	–2.339	–5.906
GDPD2	Glycerophosphodiester phosphodiesterase domain containing 2	–2.28	–2.539
NEK3	NIMA related kinase 3	–2.235	–3.583
CCDC62	Coiled-coil domain containing 62	–2.234	–3.062
ST8SIA5	ST8 aspha-N-acetyl-neuraminide alpha-2,8-sialytransferase 5	–2.232	–6.472
CHKB	Choline kinase beta	–2.219	–2.888
IL5RA	Interleukin 5 receptor subunit alpha	–2.218	–2.015
RPL10A	Ribosomal protein L10A	–2.2	–1.514
RPS13	Ribosomal protein s13	–2.191	–1.329
PIGH	Phosphatidylinositol glycan anchor biosynthesis, class H	–2.159	–2.072
LINGO4	Leucine rich repeat and Ig domain containing 4	–2.159	–5.562
CCDC152	Coiled-coil domain containing 152	–2.131	–3.069
RSRP1	Arginine/serine rich protein 1	–2.13	–1.756
ALS2CL	Als2 C-terminal like	–2.081	–1.219
B3GAT2	Beta-1,3-glucuronyltransferase 2	–2.074	–1.656
Aph1c	Aph1 homolog, gamma secretase subunit	–2.059	–3.541
CYP2C44	Cytochrome family 2, subfamily c, polypeptide 23	–2.049	–5.493
GAL	Galanin	–2.045	–1.863
SUN3	Sad1 and UNC84 domain containing 3	–2.044	–2.582
FTH1	Ferritin heavy polypeptide 1	–2.033	–1.886
PLSCR4	Phospholipid scramblase 4	–2.028	–3.39
TCF7L2	Transcription factor 7 like 2	–2.015	–2.63
PNP	Purine-nucleoside phosphorylase	–2.008	–2.019
RHBDL1	Rhomboid like 1	–1.997	–2.056
ARGLU1	Arginine and glutamate rich 1	–1.991	–1.564
GSDMC	Gasdermin C	–1.987	–5.246
OOEP	Oocyte expressed protein	–1.981	–5.338
AQP8	Aquaporin 8	–1.967	–9.629

[a]Indicates colon cancer biomarker (FDR < 0.05, fold change $>|1.5|$, IPA.

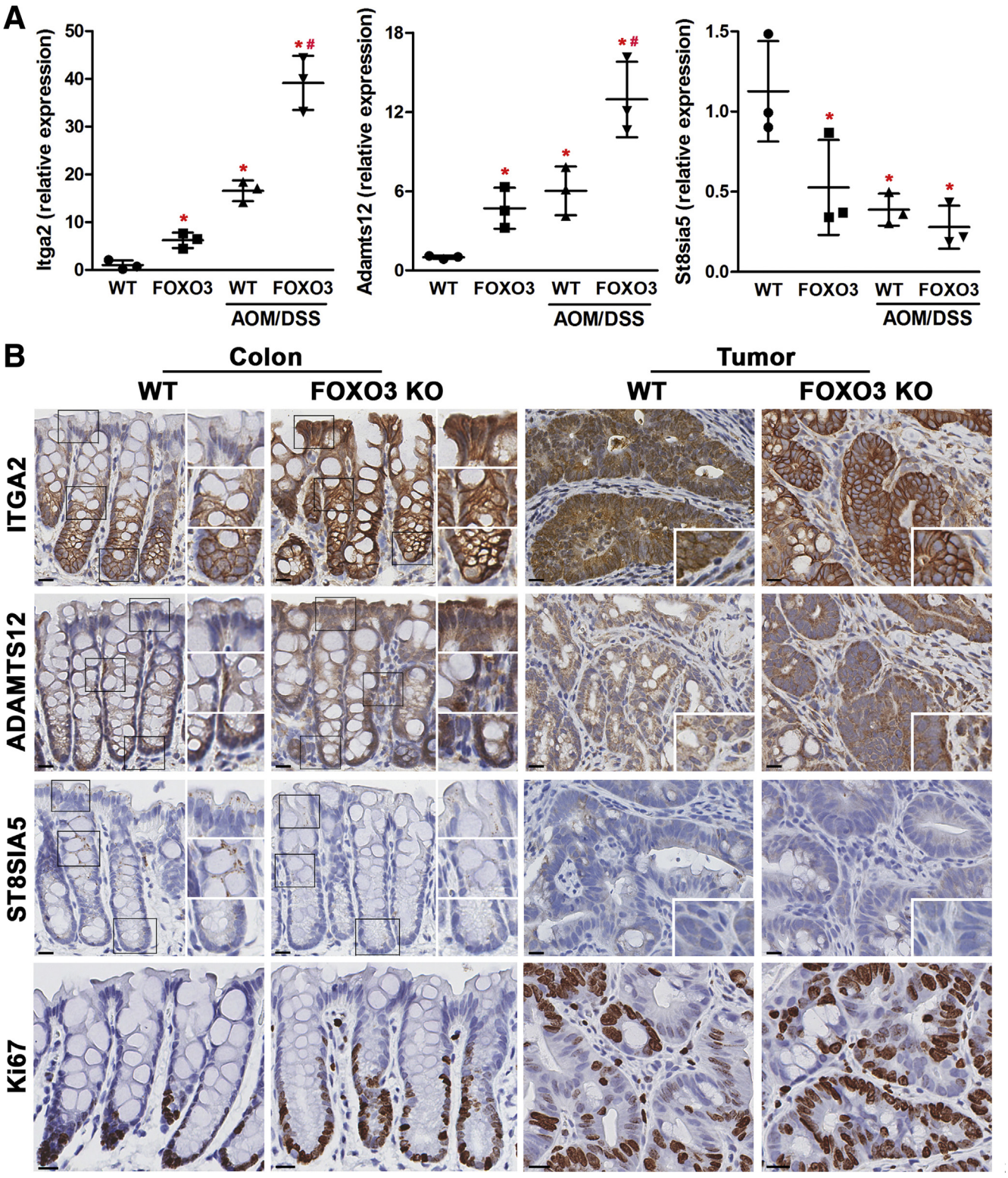

Figure 6. Altered expression of ITGA2, ADAMTS12, and ST8SIA5 transcripts in mouse colon and tumors. (*A*) Altered levels of select, novel transcripts in FOXO3 KO colon and tumors was confirmed by qPCR (n = 3 per group from 2 independent experiments; $^{*,\#}P < .05$ *relative to WT colon, $^{\#}$relative to WT tumor; analysis of variance and Student-Newman-Keuls post-test). (*B*) Immunohistostainings of ITGA2, ADAMTS12, ST8SIA5, and Ki67 in colon and tumors of WT and FOXO3 KO mice. In WT and FOXO3 KO colon, *gray boxes* represent optical zoom images from the crypt base, midsection, and apical region as displayed as panels on the right. *Insets* in tumor panels (WT and FOXO3 KO) depict higher magnification of tumor and stromal sections (representative staining from colon and tumors of 3 mice from 2 independent immunohistostainings, scale bar 25 μm).

loss of FOXO3.[15] These data demonstrate that in colon loss of FOXO3 leads to altered expression of ITGA2, ADAMTS12, and ST8SIA5 transcripts with potential roles in inflammation-mediated colon cancer progression.

Human Inflammatory Bowel Disease and Colon Cancer Progression Are Associated With Altered Expression of Novel Integrin Subunit Alpha 2, ADAM Metallopeptidase With Thrombospondin Type 1 Motif 12, and ST8 Alpha-N-Acetyl-Neuraminide Alpha-2,8-Sialyltransferase 5 Transcripts

We examined in human IBD and colon cancer patient cohorts whether altered ITGA2, ADAMTS12, and ST8SIA5 levels might play a role in their pathobiology. Similar to mouse inflammatory tumors, in IBD tissue (GSE4183) levels of both ITGA2 and ADAMTS12 transcripts were substantially increased, whereas ST8SIA5 was reduced (Figure 7*A*). In human colon cancer (TCGA), ITGA2, ADAMTS12, and ST8SIA5 expression co-occurred with established colon cancer biomarkers (data not shown), and their combined alterations including gene amplification, mutations, and mRNA/protein dysregulation were seen in 14% of colon cancer patients (Figure 7*B*). Moreover, analysis of human colon cancer transcriptomes (TCGA) indicated ITGA2 and ADAMTS12 levels were substantially increased, whereas expression of ST8SIA5 was considerably decreased compared with normal colon (Figure 7*C*; RSEM, $P < .001$). This trend of ITGA2, ADAMTS12, and ST8SIA5 expression was also found in other cancers such as esophagus, stomach, liver, lung, kidney, breast, and prostate (data not shown). Moreover, expression levels of these transcripts in human colon as shown by RNAseq (RSEM, Figure 7*C*) appear to be similar to levels observed in mouse tissues (Figure 6*B*), eg, high ITGA2, moderate ADAMTS12, and low ST8SIA5 expression. Ultimately, in human colon cancer, increased ITGA2 and ADAMTS12 as well as decreased ST8SIA5 were associated with poor patient survival (Figure 7*D*). These data indicate that these novel transcripts dependent on loss of FOXO3 have altered expression in human IBD and colon cancer possibly implicating their role in progression of both pathobiologies.

In Human Colon Cancer Cells Forkhead Box O3 Silencing Mediates Increased Integrin Subunit Alpha 2 Levels Leading to Increased Proliferation

Next, we assessed whether expression of these novel transcripts occurred in colon cancer cells, was FOXO3-dependent, and had any possible role in cancer progression. Emerging studies showed that although ITGA2 and ADAMTS12 are found in fibroblasts,[41,42] their expression and potential roles in colonic cells are not examined. Thus, we generated human colon cancer HCT116 cells with FOXO3-specific knockdown using shRNA (shFOXO3) under inducible doxycycline (dox)-inducible promoter. Among several stable transfected clones, we selected those that after dox-treatment showed reduction in endogenous FOXO3 (mRNA and protein) levels (50% ± 4%) (Figure 8*A* and *C*). In HCT116 cells, with or without shFOXO3, levels of ADAMTS12 and ST8SIA5 were insignificant, as assessed by qPCR and immunoblot (data not shown), most likely because of low baseline expression (ST8SIA5) or high methylation status (ADAMTS12)[41] of these genes in colon cancer cells. However, ITGA2, expressed in colon cancer HCT116 cells, was increased more than 2.5-fold in response to 50% FOXO3 knockdown (Figure 8*B* and *C*). Moreover, in human colon cancer HCT116 cells silencing of ITGA2 (siRNA) led to significant reduction in cell proliferation (47% ± 2%), indicating a potential role for this gene in colon cancer cell growth (Figure 8*D*). Although further study is required to determine whether increased ITGA2 expression is directly or indirectly dependent on loss of FOXO3, these findings demonstrate colon cancer cell specific ITGA2 regulation that could facilitate elevated cancer cell growth.

Discussion

Colon cancer increased risk, progression, and resistance to chemotherapy is linked to an inflammatory microenvironment[1,3,6]; however, the mechanisms involved in inflammation promoted tumor growth are not fully understood. Here, in a mouse model of inflammation-mediated colon cancer, we identified alterations driven by loss of FOXO3 within the immune cell landscape, molecular pathways, and transcripts leading to tumor growth. In mouse colon and tumors, we validated differential expression of novel transcripts including ITGA2, ADAMTS12, and ST8SIA5 in response to FOXO3 deficiency. Their expression was similarly altered in human IBD and cancer tissues and associated with poor survival in colon cancer patients. Also, in human colon cancer cells, increased ITGA2 expression, mediated by loss of FOXO3 function, was important for cell growth. These findings provide an opportunity to pursue new mechanisms, biomarkers, and prospective targets for treatment of inflammation-mediated colon cancer.

In mouse colon, deficiency in FOXO3 led to increased tumor incidence and size in the AOM/DSS model. Similar to human inflammatory colon cancer samples,[32] mouse colon deficient in FOXO3 exhibited a strong presence of neutrophils, macrophages, B and T cells, and decreased NK cells. Also, FOXO3-deficient colon and tumors had notably elevated B cells relative to WT. We speculate this effect could be a direct consequence of FOXO3 deficiency in B cells leading to their proliferation and enhanced activity[10] or occurring as a result of a B-cell response to commensal bacteria because FOXO3 deficiency also activated bacterial TLR signaling. Whether this immune profile is active or inactive and possesses pro- or anti-tumor functions remains unclear; however, emerging findings in human and mouse models have revealed that individually macrophages, neutrophils, T cells, and NK cells play important roles in colon cancer progression.[3,32] For example, Jobin et al[43] demonstrated that individuals with lower NK cell activity in blood have substantially higher risk of developing colon cancer. Also, in mouse colon, macrophages polarized by commensal bacteria have been shown to stimulate inflammation and

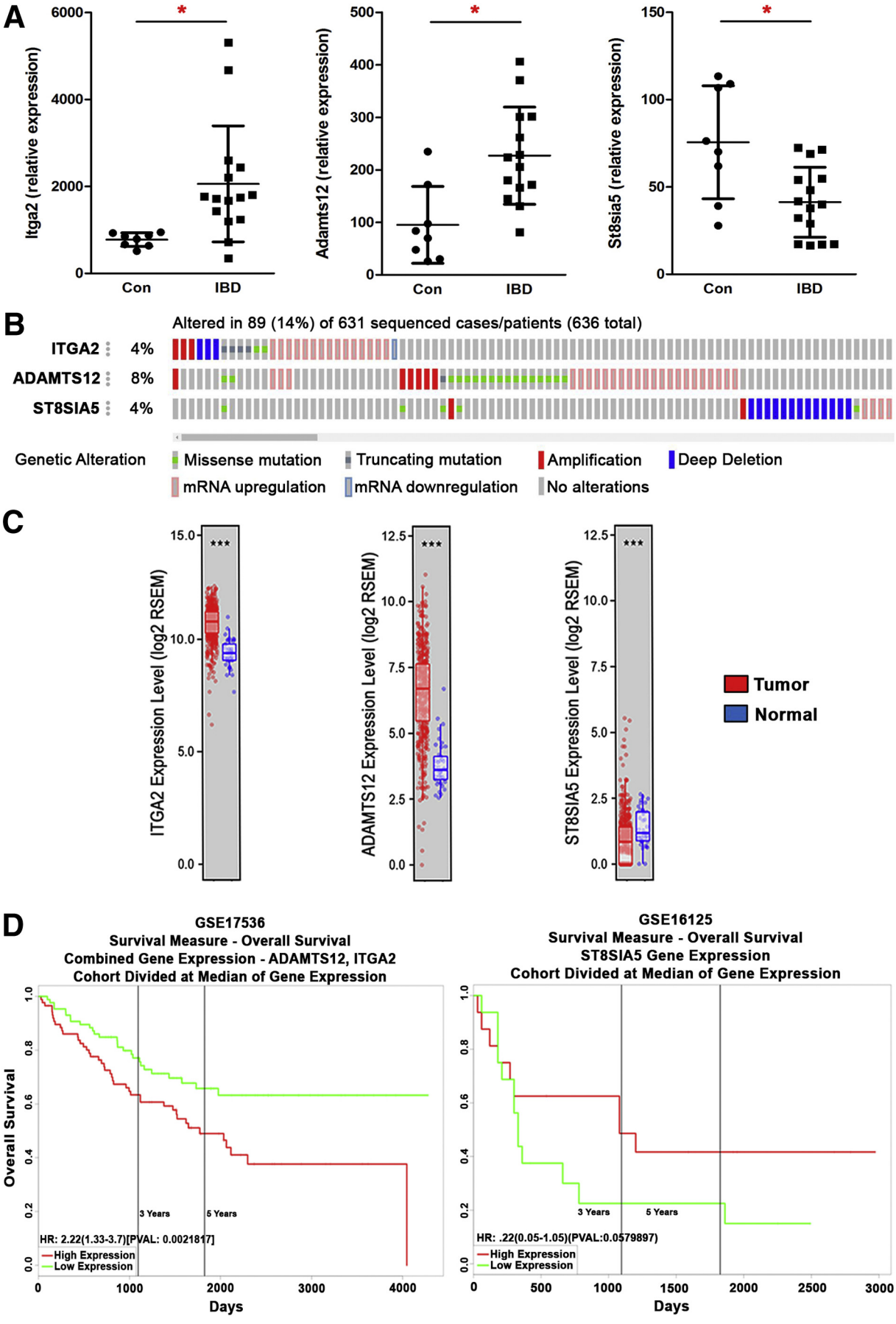
A
Itga2 (relative expression)
Adamts12 (relative expression)
St8sia5 (relative expression)
Con
IBD
B
Altered in 89 (14%) of 631 sequenced cases/patients (636 total)
ITGA2 4%
ADAMTS12 8%
ST8SIA5 4%
Genetic Alteration
Missense mutation
Truncating mutation
Amplification
Deep Deletion
mRNA upregulation
mRNA downregulation
No alterations
C
ITGA2 Expression Level (log2 RSEM)
ADAMTS12 Expression Level (log2 RSEM)
ST8SIA5 Expression Level (log2 RSEM)
Tumor
Normal
D
GSE17536
Survival Measure - Overall Survival
Combined Gene Expression - ADAMTS12, ITGA2
Cohort Divided at Median of Gene Expression
HR: 2.22(1.33-3.7)[PVAL: 0.0021817]
High Expression
Low Expression
3 Years
5 Years
Overall Survival
Days
GSE16125
Survival Measure - Overall Survival
ST8SIA5 Gene Expression
Cohort Divided at Median of Gene Expression
HR: .22(0.05-1.05)(PVAL:0.0579897)

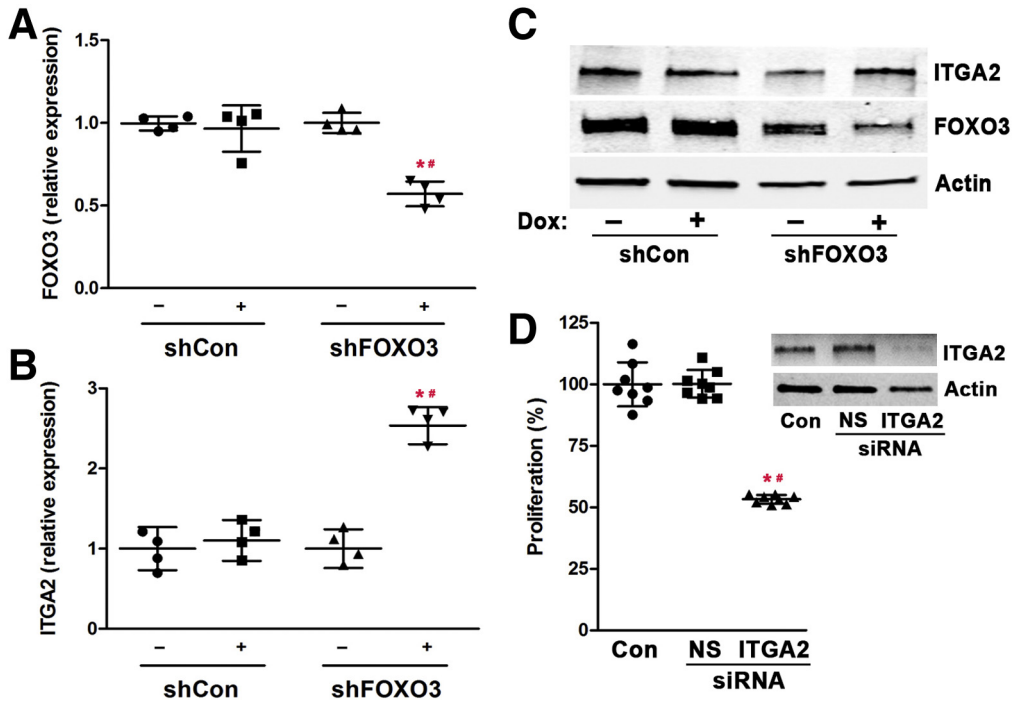

Figure 8. In human colon cancer HCT116 cells FOXO3 silencing leads to increased ITGA2 levels that promote growth. (*A*) Human colon cancer HCT116 clones with (dox)-inducible (2 μg/mL, 48 hours) FOXO3-specific shRNA (shFOXO3) were assessed for reduced FOXO3 mRNA levels (n = 4 from 2 independent experiments and clones; $^{*,\#}P < .05$, *compared with control (shCon) (-dox), #compared with shFOXO3 (-dox); analysis of variance and Student-Newman-Keuls post-test). (*B*) Increased ITGA2 expression in response to FOXO3 knockdown (shFOXO3) in colon cancer cells was determined by qPCR (n = 4 from 2 independent experiments and clones; $^{*,\#}P < .05$, *compared with shCon (-dox), #compared with shFOXO3 (-dox); analysis of variance and Student-Newman-Keuls post-test). (*C*) Immunoblot of elevated ITGA2 and reduced FOXO3 protein levels in shFOXO3 colon cancer cells (n = 4 from 2 independent experiments and clones; $^{*,\#}P < .05$, *compared with shCon (-dox), #compared with shFOXO3 (-dox); analysis of variance and Student-Newman-Keuls post-test). (*D*) MTS proliferation assay of colon cancer cells left untreated (control, Con) or transfected with non-specific scramble (NS) siRNA or ITGA2 specific siRNA (n = 8 per condition from 2 independent experiments; $^{*,\#}P < .05$, *compared with Con, #compared with NS Con; analysis of variance and Student-Newman-Keuls post-test).

cancer progression.[44] It has also been demonstrated that depletion of neutrophils with Ly6G antibodies ameliorates tumor number and size,[45] and together, molecular crosstalk between macrophages and neutrophils could promote infiltration of T cells.[46] In addition to approved immunotherapy for MSI colon cancer that stimulates T-cell antitumor function,[47] we speculate that determining the tumor functional roles of the FOXO3-dependent immune profile could lead to its targeting for more effective immunotherapeutic treatment regimens.

Functional deficiency of FOXO3 in mouse colon led to pathway activation associated with inflammatory NFκB and tumorigenic cMyc transcriptional programs as well as bacterial TLR signaling. Although activity of these transcription factors is linked to FOXO3 function,[11,14,48] the contribution of NFκB and cMyc in individual cell types in inflammation-mediated colon cancer needs to be further examined. We found increased levels of transcripts associated with inflammation and cancer, which might be directly regulated by FOXO3 or indirectly by NFκB and cMyc. Moreover, in FOXO3 KO colon, increased TLRs (level and activity) could lead to enhanced sensitivity to luminal commensal bacteria. Because bacterial products stimulate inflammation in part through loss of FOXO3 function,[12,18] our findings suggest a possible feedback between FOXO3 function and TLR signaling that may also drive inflammatory tumor growth. Together, loss of colonic FOXO3 might simultaneously orchestrate downstream signaling that could promote

Figure 7. (*See previous page*). Expression of ITGA2, ADAMTS12, and ST8SIA5 transcripts across human IBD and colon cancer. (*A*) In human IBD tissue samples, levels of ITGA2, ADAMTS12, and ST8SIA5 were significantly altered relative to normal control (GSE4183, n = 23 patient samples, Agilent Microarray Probe ID: ITGA2 (22734_at), ADAMTS12 (226997_at), ST8SIA5 (217514_at); $^{*}P < .05$ compared with healthy control, Student *t* test). (*B*) OncoPrint alteration summary of ADAMTS12, ITGA2, and ST8SIA5 in human colon cancer (TCGA) (cbioportal.org, $P < .05$). (*C* and *D*) mRNA expression of select, novel transcripts ITGA2, ADAMTS12, and ST8SIA5 were significantly altered in human colon cancer compared with matched control tissue (TCGA) (TIMER, $^{***}P < .001$ compared with normal tissue) and were associated with poor patient survival as measured by KM estimate (PROGgeneV2) ($^{*}P < .05$).

increased sensitivity to commensal bacteria and inflammation leading to cancer initiation and progression.

We identified in mouse colon a substantial number of novel transcripts that might be directly or indirectly altered because of FOXO3 functional deficiency or consequently because of activated inflammatory-tumorigenic programs including ITGA2, ADAMTS12, and ST8SIA5. In human colon cancer tissues, increased ADAMTS12 expression is found predominantly in fibroblasts,[41] and although in various human colon cancer cell lines there is lack of ADAMS12 expression because of methylation, its expression is recovered after co-culture with fibroblasts.[41] Our findings demonstrate that ADAMTS12 levels, while negligibly present in human colon cancer cells, were significantly increased (transcripts and protein) in mouse colonic cells of FOXO3 KO colon and tumors, as well as in infiltrated non-colonic cells. Furthermore, in mouse colon, ST8SIA5 protein appears to localize in select colonic cells. Although in human colon cancer cells ST8SIA5 expression level was negligible, its further decrease in human colon cancer appeared to be critical for poor patient survival. Moreover, emerging findings have revealed in IBD patients that genome-wide variants in ST8SIA5 are associated with response to select therapy[49]; in addition, an ST8SIA5 family member (ST8SIA1) has been recently used in immunotherapeutic vaccine delivery to stimulate NK cell activity against tumor growth.[50] Thus, although ST8SIA5 levels might be low in colon, recovery of its levels/function might have potential therapeutic benefits in IBD and colon cancer. Moreover, ITGA2 abundance was found not only in mouse colonic cells and tumors but also in human colon cancer cells and was critical for cell growth. Increased ITGA2 has recently been implicated in fibroblast-driven inflammatory rheumatoid arthritis,[42] resistance of gastric cancer cells to apoptosis,[51] and human colon cancer metastasis.[52] We speculate that in colon elevated ITGA2 exerts multiple functions in colonic and non-colonic cells to facilitate inflammation-mediated cancer pathobiology. Moreover, because we found that partial reduction in FOXO3 levels in human colon cancer cells led to significantly increased ITGA2 expression, we speculate that in human colon SNPs in the FOXO3 gene might have significant implications in driving gene expression involved in inflammatory and cancer progression. In addition, whether these novel transcripts are directly or indirectly regulated by FOXO3 is unclear; they could act as novel functional regulators in inflammation-mediated colon cancer progression.

In conclusion, FOXO3 deficiency in a mouse model of inflammation-mediated colon cancer increases colonic tumor burden. Moreover, loss of FOXO3 also leads to elevated intracellular lipids,[53] an emerging aspect of metabolic reprogramming associated with inflammation and colon cancer,[54] suggesting FOXO3's metabolic function may also be involved in these disease processes. These findings underline novel FOXO3-dependent regulators that could serve as biomarkers and prospective new targets for treatment of colon cancer. Overall, understanding the immune landscape and molecular pathways of inflammation-mediated colon cancer highlights a future direction for precision diagnostics and personalized treatments.

References

1. Colotta F, Allavena P, Sica A, Garlanda C, Mantovani A. Cancer-related inflammation, the seventh hallmark of cancer: links to genetic instability. Carcinogenesis 2009; 30:1073–1081.
2. Pietrzyk L, Torres A, Maciejewski R, Torres K. Obesity and obese-related chronic low-grade inflammation in promotion of colorectal cancer development. Asian Pac J Cancer Prev 2015;16:4161–4168.
3. Elinav E, Nowarski R, Thaiss CA, Hu B, Jin C, Flavell RA. Inflammation-induced cancer: crosstalk between tumours, immune cells and microorganisms. Nat Rev Cancer 2013;13:759–771.
4. Itzkowitz SH, Yio X. Inflammation and cancer IV: colorectal cancer in inflammatory bowel disease—the role of inflammation. Am J Physiol Gastrointest Liver Physiol 2004;287:G7–G17.
5. Rubin DC, Shaker A, Levin MS. Chronic intestinal inflammation: inflammatory bowel disease and colitis-associated colon cancer. Front Immunol 2012;3:107.
6. Fridman WH, Pages F, Sautes-Fridman C, Galon G. The immune contexture in human tumours: impact on clinical outcome. Nat Rev Cancer 2012;12:298–306.
7. Biggs WH 3rd, Cavenee WK, Arden KC. Identification and characterization of members of the FKHR (FOX O) subclass of winged-helix transcription factors in the mouse. Mamm Genome 2001;12:416–425.
8. Coomans de Brachene A, Demoulin JB. FOXO transcription factors in cancer development and therapy. Cell Mol Life Sci 2016;73:1159–1172.
9. Tothova Z, Gilliland DG. FoxO transcription factors and stem cell homeostasis: insights from the hematopoietic system. Cell Stem Cell 2007;1:140–152.
10. Peng SL. Foxo in the immune system. Oncogene 2008; 27:2337–2344.
11. Lin L, Hron JD, Peng SL. Regulation of NF-kappaB, Th activation, and autoinflammation by the forkhead transcription factor Foxo3a. Immunity 2004;21:203–213.
12. Lee JC, Espeli M, Anderson CA, Linterman MA, Pocock JM, Williams NJ, Roberts R, Viatte S, Fu B, Peshu N, Hien TT, Phu NH, Wesley E, Edwards C, Ahmad T, Mansfield JC, Gearry R, Dunstan S, Williams TN, Barton A, Vinuesa CG, UK IBD Genetics ConsortiumParkes M, Lyons PA, Smith K. Human SNP links differential outcomes in inflammatory and infectious disease to a FOXO3-regulated pathway. Cell 2013;155:57–69.
13. Bullock MD, Bruce A, Sreekumar R, Curtis N, Cheung T, Reading I, Primrose JN, Ottensmeier C, Packham GK, Thomas G, Mirnezami AH. FOXO3 expression during colorectal cancer progression: biomarker potential reflects a tumour suppressor role. Br J Cancer 2013; 109:387–394.
14. Snoeks L, Weber CR, Wasland K, Turner JR, Vainder C, Qi W, Savkovic SD. Tumor suppressor FOXO3

participates in the regulation of intestinal inflammation. Lab Invest 2009;89:1053–1062.
15. Qi W, Weber CR, Wasland K, Wasland K, Roy H, Wali R, Joshi S, Savkovic SD. Tumor suppressor FOXO3 mediates signals from the EGF receptor to regulate proliferation of colonic cells. Am J Physiol Gastrointest Liver Physiol 2011;300:G264–G272.
16. Greten FR, Eckmann L, Greten TF, Park JM, Li ZW, Egan LJ, Kagnoff MF, Karin M. IKKbeta links inflammation and tumorigenesis in a mouse model of colitis-associated cancer. Cell 2004;118:285–296.
17. Fellmann C, Hoffmann T, Sridhar V, Hopfgartner B, Muhar M, Roth M, Lai DY, Barbosa IA, Kwon JS, Guan Y, Sinha N, Zuber J. An optimized microRNA backbone for effective single-copy RNAi. Cell Rep 2013; 5:1704–1713.
18. Snoeks L, Weber CR, Turner JR, Bhattacharyya M, Wasland K, Savkovic SD. Tumor suppressor Foxo3a is involved in the regulation of lipopolysaccharide-induced interleukin-8 in intestinal HT-29 cells. Infect Immun 2008;76:4677–4685.
19. Penrose HM, Heller S, Cable C, Nakhoul H, Baddoo M, Flemington E, Crawford SE, Savkovic SD. High-fat diet induced leptin and Wnt expression: RNA-sequencing and pathway analysis of mouse colonic tissue and tumors. Carcinogenesis 2017;38:302–311.
20. Heller S, Penrose HM, Cable C, Biswas D, Nakhoul H, Baddoo M, Flemington E, Crawford SE, Savkovic SD. Reduced mitochondrial activity in colonocytes facilitates AMPKalpha2-dependent inflammation. FASEB J 2017; 31:2013–2025.
21. Kerr TA, Ciorba MA, Matsumoto H, Davis VR, Luo J, Kennedy S, Xie Y, Shaker A, Dieckgraefe BK, Davidson NO. Dextran sodium sulfate inhibition of real-time polymerase chain reaction amplification: a poly-A purification solution. Inflamm Bowel Dis 2012;18:344–348.
22. Barrett T, Wilhite SE, Ledoux P, Evangelista C, Kim IF, Tomashevsky M, Marshall KA, Phillippy KH, Sherman PM, Holko M, Yefanov A, Lee H, Zhang N, Robertson CL, Serova N, Davis S, Soboleva A. NCBI GEO: archive for functional genomics data sets—update. Nucleic Acids Res 2013;41:D991–D995.
23. Cancer Genome Atlas Network. Comprehensive molecular characterization of human colon and rectal cancer. Nature 2012;487:330–337.
24. Gao J, Aksoy BA, Dogrusoz U, Dresdner G, Gross B, Sumer SO, Sun Y, Jacobsen A, Sinha R, Larsson E, Cerami E, Sander C, Schultz N. Integrative analysis of complex cancer genomics and clinical profiles using the cBioPortal. Sci Signal 2013;6:pl1.
25. Cerami E, Gao J, Dogrusoz U, Gross BE, Sumer SO, Aksoy BA, Jacobsen A, Byrne CJ, Heuer ML, Larsson E, Antipin Y, Reva B, Goldberg AP, Sander C, Schultz N. The cBio cancer genomics portal: an open platform for exploring multidimensional cancer genomics data. Cancer Discov 2012;2:401–404.
26. Li B, Dewey CN. RSEM: accurate transcript quantification from RNA-Seq data with or without a reference genome. BMC Bioinformatics 2011;12:323–339.
27. Newman AM, Liu CL, Green MR, Gentles AJ, Feng W, Xu Y, Hoang CD, Diehn M, Alizadeh AA. Robust enumeration of cell subsets from tissue expression profiles. Nat Methods 2015;12:453–457.
28. Li B, Severson E, Pignon JC, Zhao H, Li T, Novak J, Jiang P, Shen H, Aster JC, Rodig S, Signoretti S, Liu JS, Liu XS. Comprehensive analyses of tumor immunity: implications for cancer immunotherapy. Genome Biol 2016;17:174.
29. Subramanian A, Tamayo P, Mootha VK, Mukherjee S, Ebert BL, Gillette MA, Paulovich A, Pomeroy SL, Golub TR, Lander ES, Mesirov JP. Gene set enrichment analysis: a knowledge-based approach for interpreting genome-wide expression profiles. Proc Natl Acad Sci U S A 2005;102:15545–15550.
30. Burgering BM, Kops GJ. Cell cycle and death control: long live Forkheads. Trends Biochem Sci 2002; 27:352–360.
31. Samuels Y, Ericson K. Oncogenic PI3K and its role in cancer. Curr Opin Oncol 2006;18:77–82.
32. Grivennikov SI, Greten FR, Karin M. Immunity, inflammation, and cancer. Cell 2010;140:883–899.
33. Kim HJ, Kang HJ, Lee H, LOee ST, Yu MH, Kim H, Lee C. Identification of S100A8 and S100A9 as serological markers for colorectal cancer. J Proteome Res 2009; 8:1368–1379.
34. Cho KH, Baek S, Sung MH. Wnt pathway mutations selected by optimal beta-catenin signaling for tumorigenesis. FEBS Lett 2006;580:3665–3670.
35. Storz P, Doppler H, Copland JA, Simpson KJ, Toker A. FOXO3a promotes tumor cell invasion through the induction of matrix metalloproteinases. Mol Cell Biol 2009; 29:4906–4917.
36. Fukata M, Abreu MT. TLR4 signalling in the intestine in health and disease. Biochem Soc Trans 2007; 35:1473–1478.
37. Sanchez-Munoz F, Fonseca-Camarillo G, Villeda-Ramirez MA, Miranda-Perez E, Mendivil EJ, Barreto-Zuniga R, Uribe M, Bojalil R, Dominguez-Lopez A, Yamamoto-Furusho JK. Transcript levels of Toll-like receptors 5, 8 and 9 correlate with inflammatory activity in ulcerative colitis. BMC Gastroenterol 2011; 11:138.
38. Kapp TG, Rechenmacher F, Sobahi TR, Kessier H. Integrin modulators: a patent review. Expert Opin Ther Pat 2013;23:1273–1295.
39. Wei J, Richbourgh B, Jia T, Liu C. ADAMTS-12: a multifaced metalloproteinase in arthritis and inflammation. Mediators Inflamm 2014;2014:649718.
40. Wang XQ, Sun P, Paller AS. Ganglioside modulation regulates epithelial cell adhesion and spreading via ganglioside-specific effects on signaling. J Biol Chem 2002;277:40410–40419.
41. Moncada-Pazos A, Obaya AJ, Fraga MF, Viloria CG, Capella G, Gausachs M, Esteller M, Lopez-Otin C, Cal S. The ADAMTS12 metalloprotease gene is epigenetically silenced in tumor cells and transcriptionally activated in the stroma during progression of colon cancer. J Cell Sci 2009;122:2906–2913.

42. Peters MA, Wendholt D, Strietholt S, Frank S, Pundt N, Korb-Pap A, Joosten LA, van den Berg WB, Kollias G, Eckes B, Pap T. The loss of alpha2beta1 integrin suppresses joint inflammation and cartilage destruction in mouse models of rheumatoid arthritis. Arthritis Rheum 2012;64:1359–1368.
43. Jobin G, Rodriguez-Suarez R, Betito K. Association between natural killer cell activity and colorectal cancer in high-risk subjects undergoing colonoscopy. Gastroenterology 2017;153:980–987.
44. Yang Y, Wang X, Huycke T, Moore DR, Lightfoot SA, Huycke MM. Colon macrophages polarized by commensal bacteria cause colitis and cancer through the bystander effect. Transl Oncol 2013;6:596–606.
45. Shang K, Bai YP, Wang C, Wang Z, Gu HY, Du X, Zhou XY, Zheng CL, Chi YY, Mukaida N, Li YY. Crucial involvement of tumor-associated neutrophils in the regulation of chronic colitis-associated carcinogenesis in mice. PLoS One 2012;7:e51848.
46. Rahat MA, Coffelt SB, Granot Z, Muthana M, Amedei A. Macrophages and neutrophils: regulation of the inflammatory microenvironment in autoimmunity and cancer. Mediators Inflamm 2016;2016:5894347.
47. Boland PM, Ma WW. Immunotherapy for colorectal cancer. Cancers (Basel) 2017;9.
48. Delpuech O, Griffiths B, East P, Essafi A, Lam EW, Burgering B, Downward J, Schulze A. Induction of Mxi1-SR alpha by FOXO3a contributes to repression of Myc-dependent gene expression. Mol Cell Biol 2007; 27:4917–4930.
49. Moran CJ, Huang H, Rivas M, Kaplan JL, Daly MJ, Winter HS. Genetic variants in cellular transport do not affect mesalamine response in ulcerative colitis. PLoS One 2018;13:e0192806.
50. Eby JM, Barse L, Henning SW, Rabelink MJ, Klarquist J, Gilbert ER, Hammer AM, Fernandez MF, Yung N, Khan S, Miller HG, Kessler ER, Garrett-Mayer E, Dilling DF, Hoeben RC, Le Poole IC. Alpha-N-acetylneuraminide alpha-2,8-sialyltransferase 1 can support immune responses toward tumors overexpressing ganglioside D3 in mice. Cancer Immunol Immunother 2017;66:63–75.
51. Chuang YC, Wu HY, Lin YL, Tzou SC, Chuang CH, Jian TY, Chen PR, Chang YC, Lin CH, Huang TH, Wang CC, Chan YL, Liao KW. Blockade of ITGA2 induces apoptosis and inhibits cell migration in gastric cancer. Biol Proced Online 2018;20:10.
52. Yang Q, Bavi P, Wang JY, Roehrk MH. Immuno-proteomic discovery of tumor tissue autoantigens identifies olfactomedin 4, CD11b, and integrin alpha-2 as markers of colorectal cancer with liver metastases. J Proteomics 2017;168:53–65.
53. Qi W, Fitchev PS, Cornwell ML, Greenberg J, Cabe M, Weber CR, Roy HK, Crawford SE, Savkovic SD. FOXO3 growth inhibition of colonic cells is dependent on intraepithelial lipid droplet density. J Biol Chem 2013; 288:16274–16281.
54. Cotte AK, Aires V, Fredon M, Limagne E, Derangere V, Thibaudin M, Humblin E, Scagliarini A, de Barros JP, Hillon P, Ghiringhelli F, Delmas D. Lysophosphatidylcholine acyltransferase 2-mediated lipid droplet production supports colorectal cancer chemoresistance. Nat Commun 2018;9:322.

Received March 13, 2018. Accepted October 9, 2018.

Correspondence
Address correspondence to: Suzana Savkovic, PhD, Tulane University, Department of Pathology and Laboratory Medicine; 1430 Tulane Avenue SL-79, New Orleans, Louisiana 70112. e-mail: ssavkovi@tulane.edu; fax: (504) 988-7389.

Author contributions
H.P. and S.D.S.: conception and design of research; H.P., M.B., S.H., C.C., and A.B.H. performed experiments; H.P., S.H., H.N., N.U., S.B.L., and S.D.S. analyzed data; H.P. and S.D.S. interpreted results of experiments; H.P. prepared figures; E.F.F., M.E.B, S.E.C, and S.D.S. approved final version of manuscript.

Conflicts of interest
This author discloses the following: Suzana D. Savkovic discloses ownership in Pegasus Biosolution, LLC. The remaining authors disclose no conflicts.

Funding
Supported by NIH awards RO1CA160809 and P01CA214091.